ResearchGate

See discussions, stats, and author profiles for this publication at: https://www.researchgate.net/publication/387748372

Functional Analysis of Quinovic Acid Derivatives from Sarcocephalus pobeguinii as Inhibitors of Hepatitis C Virus NS3/4A Protease

Article · March 2025

DOI: 10.1016/j.prerep.2024.100026

CITATIONS
0

READS
116

12 authors, including:

Arnaud Fondjo Kouam
University of Buea
23 PUBLICATIONS **106** CITATIONS
SEE PROFILE

Aristide Mfifen Munvera
University of Yaoundé I
19 PUBLICATIONS **101** CITATIONS
SEE PROFILE

Elisabeth Zeuko´o Menkem
University of Buea
79 PUBLICATIONS **642** CITATIONS
SEE PROFILE

Fredy Brice Nemg Simo
University of Yaoundé I
46 PUBLICATIONS **403** CITATIONS
SEE PROFILE

All content following this page was uploaded by Arnaud Fondjo Kouam on 06 January 2025.

The user has requested enhancement of the downloaded file.

Pharmacological Research â€“ Reports xxx (xxxx) 100026

Contents lists available at ScienceDirect

Pharmacological Research â€“ Reports

journal homepage: www.elsevier.com

Journal Cover Image

Functional analysis of quinovic acid derivatives from *Sarcocephalus pobeguinii* as inhibitors of hepatitis C virus NS3/4A protease

Arnaud Fondjo Kouam [a, c, 1, *], Aristide Mfifen Munvera [b], Jordas Casares Tchana Tchamba [c], Elisabeth Menkem Zeuko'o [a], Armelle Gaelle Kwesseu Fepa [c], Brice Fredy Nemg Simo [c], Felicité Syntia Douanla Somene [d], Armel Jackson Seukep [a], Pierre Mkounga [b], Jules Clément Nguedia Assob [a], Frédéric Nico Njayou [c], Paul Fewou Moundipa [c]

[a] *Medical Research and Applied Biochemistry Laboratory, Department of Biomedical Sciences, Faculty of Health Sciences, University of Buea, PO Box 63, Buea, Cameroon*
[b] *Department of Organic Chemistry, Faculty of Science, University of Yaoundé 1, PO Box 812, Yaoundé, Cameroon*
[c] *Laboratory of Pharmacology and Toxicology, Department of Biochemistry, Faculty of Science, University of Yaoundé 1, PO Box 812, Yaoundé, Cameroon*
[d] *Department of Nursing Sciences, Faculty of Health Sciences, University of Buea, PO Box 63, Buea, Cameroon*

ARTICLE INFO

Keywords:
Hepatitis C virus
S. pobeguinii
Quinovic acid and derivatives
Inhibitors
HCV-NS3/4 A protease
HCV replication

ABSTRACT

This study assessed compounds from *Sarcocephalus pobeguinii* as potential inhibitors of HCV-NS3/4 A. Ten compounds isolated from *S. pobeguinii* were initially screened for their inhibitory activity against HCV-NS3/4 A through the fluorescence resonance energy transfer assay. The 50 % inhibitory concentration (IC_{50}) and the inhibition mechanism of active compounds were determined through concentration-response and enzyme-kinetics studies, respectively. The physical interactions between the enzyme and inhibitors were analyzed by thermal shift assay and surface plasmon resonance, while molecular interactions were predicted using molecular docking. The antiviral activity of the hit compounds was tested in a cell-based assay. Three inhibitors of HCV-NS3/4 A: Quinovic acid, Quinovic acid 3-O-[α-D-quinovopyranoside], and Quinovic acid 3-O-[β-D-quinovopyranoside] with IC_{50} in the micromolar range were successfully identified. They displayed their inhibitory activity through a non-competitive inhibition mechanism and bound to the HCV-NS3/4 A protease in a real-time manner through 1:1 binding and steady-state affinity models, inducing its instability by lowering its melting temperature. The lead compounds effectively inhibited HCV replication at non-toxic concentrations. These results contribute to the valorization of *S. pobeguinii* as a potential source of efficient inhibitors to reinforce the current therapeutic arsenal for the treatment of HCV infection.

1. Introduction

The blood-borne pathogen, hepatitis C virus (HCV) is a major cause of the inflammation in the liver. The World Health Organization estimates that 58 million individuals are chronically infected, with almost 1.5 million new cases recorded each year [1]. Sub-Saharan nations are more affected by HCV, with a prevalence ranging from 3.6 % to 7.1 %, in contrast to western countries where the infection rate is less than 1 % [2]. About 30 % of afflicted individuals can eradicate the infection without any medication. The remaining 70 % experience persistent infections, which may progress to cirrhosis, and eventually hepatocellular cancer. Indeed, cirrhosis and primary liver cancer are linked to approximately 290,000 HCV-related deaths reported each year [1].

During hepatocyte infection, HCV replicates by synthesizing a precursor polyprotein, which is subsequently processed into a variety of functional proteins by the host and viral proteases. These proteins are categorized as structural (Core, Envelope E1 and E2, P7) and non-structural (NS) proteins, including NS2, NS3, NS4A, NS4B, NS5A, and NS5B. [3–5]. Among the latter, NS3 is a dual enzyme that exhibits both serine-protease and helicase activities. In addition to its function in viral replication via HCV RNA unwinding, NS3 is also accountable for the cleavage and release of others NS protein from the precursor polyprotein [6]. Additionally, NS3 contributes to evading the host's innate im-

* Corresponding author at: Medical Research and Applied Biochemistry Laboratory, Department of Biomedical Sciences, Faculty of Health Sciences, University of Buea, PO Box 63, Buea, Cameroon.
E-mail addresses: arnaudkouam@yahoo.fr, kouam.fondjo@ubuea.cm (A.F. Kouam), seukep.armel@ubuea.cm (A.J. Seukep).
[1] ORCID: 0000–0002-2629–6394

https://doi.org/10.1016/j.prerep.2024.100026
Received 31 August 2024; Received in revised form 31 December 2024; Accepted 31 December 2024
2950-2004/© 2022

CORRECTED PROOF

Note: Low-resolution images were used to create this PDF. The original images will be used in the final composition.

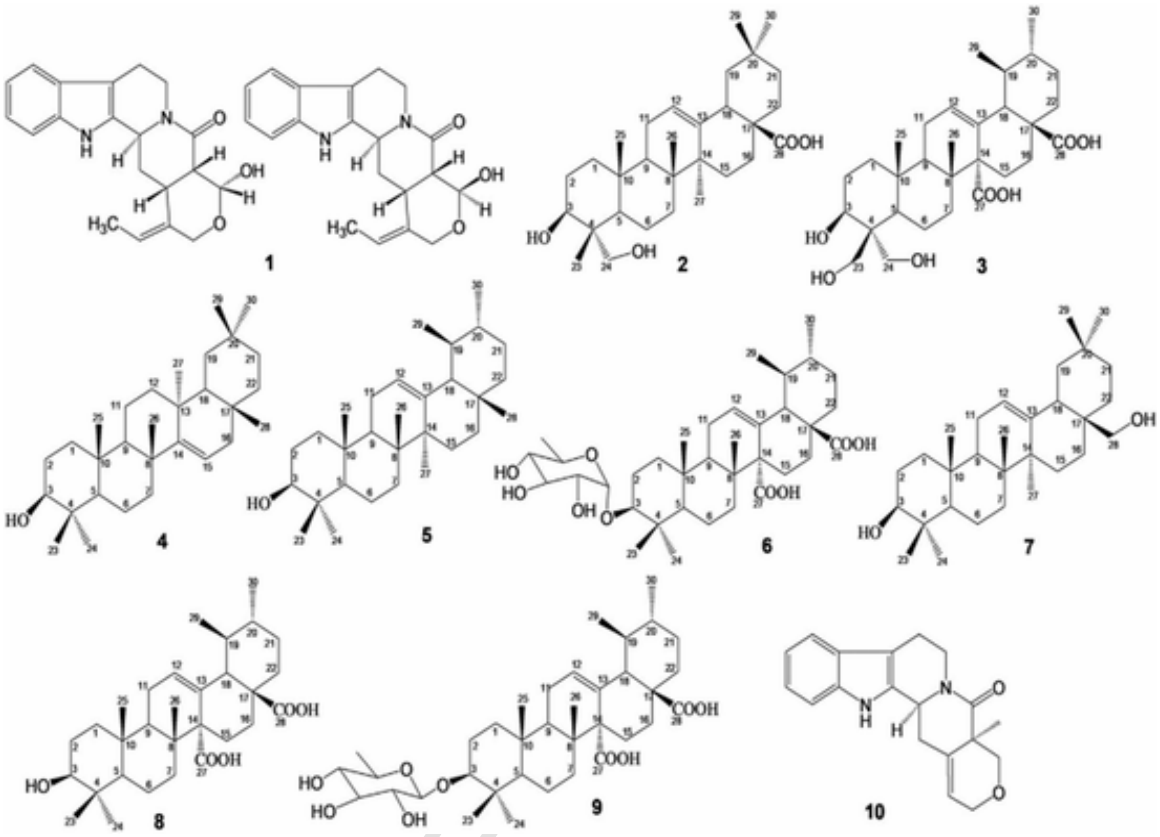

Fig. 1. Chemical structures of the studied compounds from *S. Pobeguinii.* (1): Mixture of Nauclealatifoline G and naucleofficine D; (2): Hederagenin; (3): Chletric acid; (4): Taraxerol; (5): α-amyrin (3β-hydroxy-urs-12-en-3-ol); (6): Quinovic acid 3-O-[α-D-quinovopyranoside]; (7): Erythrodiol; (8): Quinovic acid; (9): Quinovic acid 3-O-[β-D-quinovopyranoside]; (10): Latifoliamide *C*.

mune response by using its proteolytic activity to inactivate several antiviral proteins that may block the replication [7,8]. Another HCV protein is NS4A, which forms a complex with NS3 and serves as a coenzyme, thereby enhancing its activities [9,10]. Given its fundamental functions, the NS3/4 A complex is considered an important drug target, therefore contributing to the development of the current class of molecules for HCV treatment, known as direct-acting antiviral agents (DAAs). First Food and Drug Administration-approved DAAs include Boceprevir, Telaprevir, and Danoprevir, all of which are inhibitors of the NS3/4 A protease [11–14]. Although DAAs can effectively cure over 90 % of sick persons, there are barriers to early detection and treatment, especially in low-income countries where the high prevalence is associated with poverty and weak socioeconomic conditions [1]. Also, no vaccine is currently approved, and the use of DAAs could be associated with the development of resistance, as was the case with Boceprevir and Telaprevir [15]. Therefore, a search for novel anti-HCV compounds to consolidate the current healing drugs in treating HCV infection is warranted.

The role of medicinal plants in supplying modern pharmacies with bioactive compounds capable of treating human illness is well established. Among such plants, *Sarcocephalus pobeguinii*, belonging to the Rubiaceae family, is traditionally used for the treatment of several diseases, including malaria, gonorrhea, and diabetes. The antiproliferative properties of various extracts *of S. pobeguinii* against different human cancer cell lines has been reported [16]. Also, several molecules isolated from its fruits, leaves, and bark, including Quinovic acid and its derivatives, displayed potent anti-proliferative and anti-inflammatory effects [17]. However, no data on the antiviral effects of these compounds has been reported. In the contribution to unveiling bioactive molecules from natural resources, the identification of potential inhibitors of HCV NS3/4A protease bearing an anti-HCV inhibitory effect using compounds isolated from *S. pobeguinii* was the goal of this investigation.

2. Materials and methods

2.1. Reagents

Recombinant HCV NS3/4A protease genotype 1b (Cat. Number AS-61017–10) and the fluorogenic peptide substrate Ac-Asp-Glu-Asp (EDANS)-Glu-Glu-Abu-ψ-[COO]-Ala-Ser-Lys(DABCYL)- NH2 (HCV Protease FRET (RET-S1) Substrate Cat. Number AS-22991–50) were obtained from Eurogentec (Liege, Belgium) and Anaspec (Anaspec Inc., San Jose, CA) respectively. Boceprevir (BCP) was obtained from SelleckChem (Beijing, China). Thiazolyl Blue Tetrazolium Bromide was obtained from Sigma-Aldrich; Gaussia Luciferase Assay Kit and 5x Renilla Lysis buffer were obtained from NEW ENGLAND BioLabs and Promega respectively; Mouse monoclonal antibody anti-HCV core protein and Alexa-Fluor-488 goat antibody anti-mouse were supplied by Thermo Fisher Scientific (Rockford, USA). The others reagent used in this study were of analytical grade.

2.2. Studied phytochemical compounds from S. pobeguinii

Ten compounds (Fig. 1) known as: Mixture of Nauclealatifoline G and naucleofficine D (1), hederagenin (2), chletric acid (3), taraxerol (4), α-amyrin (3β-hydroxy-urs-12-en-3-ol) (5), quinovic acid 3-O-[α-D-quinovopyranoside] (6), erythrodiol (7), quinovic acid (8), quinovic

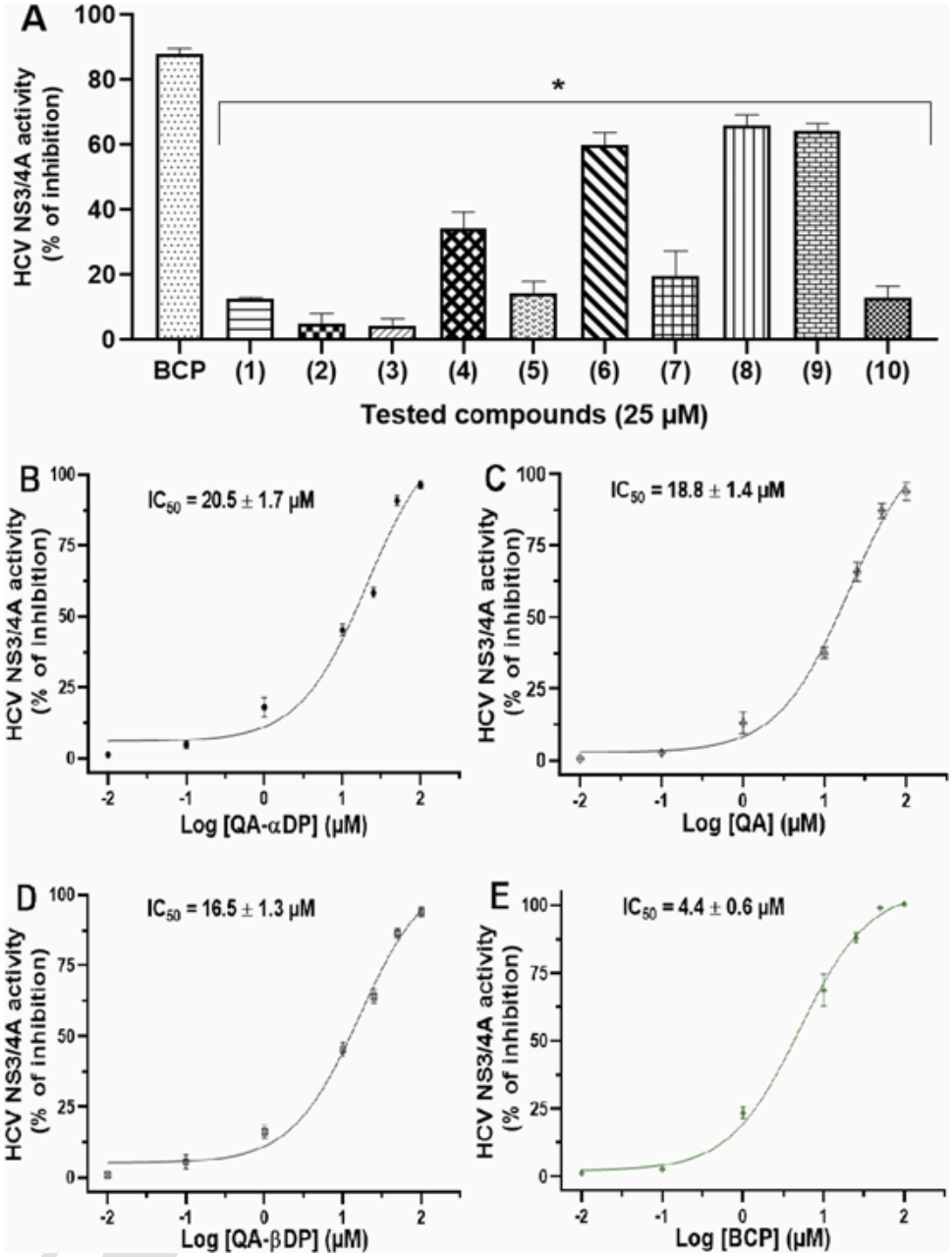

Fig. 2. Inhibitory effect of isolated compounds from *S. Pobeguinii* on the proteolytic activity of HCV NS3/4 A. (A): Initial screening of compounds from *S. Pobeguinii* tested at 25 µM on the activity of HCV NS3/4 A. (B), (C), (D) and (E): Concentration-response curve of QA, QA-αDP, QA-βDP and Boceprevir respectively. Data are means ± SD of three independent assays in triplicate *(n = 3)*. ANOVA summary: F(DFn, DFd) = F(10, 22) = 181.1, P<0.0001 (Fig. 2A).*values significantly (P<0.05) different when compared to Boceprevir using Bonferroni's test. IC_{50}: 50 % inhibitory concentration. (1): mixture of Nauclealatifoline G and naucleofficine D; (2): hederagenin; (3): chletric acid; (4): taraxerol; (5): α-amyrin (3β-hydroxy-urs-12-en-3-ol); (6) or QA-αDP: quinovic acid 3-O-[α-D-quinovopyranoside]; (7): erythrodiol; (8) or QA: quinovic acid; (9) or QA-βDP: quinovic acid 3-O-[β-D-quinovopyranoside]; (10): latifoliamide C.

acid 3-O-[β-D-quinovopyranoside] (9) and latifoliamide C (10) were tested in this study. They were previously isolated from the fruits, leaves, and bark of *S. pobeguinii* by our research group using various extraction and chromatographic techniques and their chemical structures determined through spectroscopic methods including 1^{H} and 13^{C} nuclear magnetic resonance [17].

2.3. Cells and virus strains

Human hepatoma cell line Huh7.5 was used. They were cultured in high glucose DMEM medium (Dulbecco's Modified Eagle's Medium) containing 10 % fetal bovine serum at 37°C in an atmosphere of 5 % CO_2. A derivative of the pFL-J6/JFH-1 plasmid coding for the complete viral genome of a HCV genotype 2a [18], Jc1/GLuc2A plasmid harboring *Gaussia princeps*' luciferase gene was used to generate infectious HCV-cell culture derived particles (HCVcc) tested in this study [19]. The detailed procedure regarding the *in vitro* transcription followed by the transfection of naïve Huh7.5 cells to produce the infectious HCVcc particles can be found from our previous study [20].

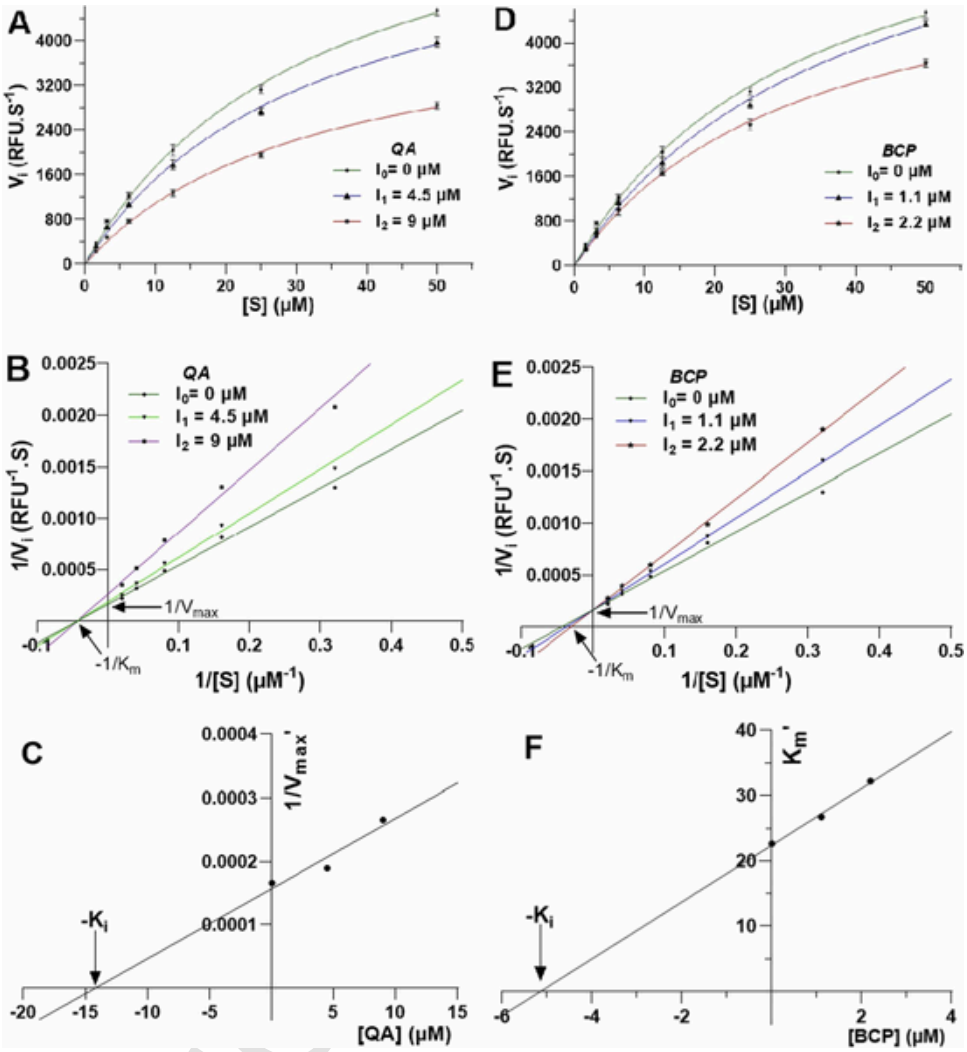

Fig. 3. Inhibition mechanism of QA acid and BCP on the proteolytic activity of HCV NS3/4 A. A and D: Michaelis-Menten plot; B and E: Lineweaver-Burk plot; C (1/Vmax' = f[I]) and F (Km' = f[I]): Secondary plot for the determination of the inhibition constant (Ki) respectively for QA and BCP.

2.4. Assessment of compounds from S. pobeguinii as potential inhibitor of HCV NS3/4A

2.4.1. Initial screening of compounds from S. pobeguinii as potential inhibitor of HCV NS3/4A proteolytic activity

The isolated compounds and Boceprevir, serving as reference inhibitor were all dissolved in DMSO and tested at the final concentration of 25 µM using the Fluorescence Resonance Energy Transfer (FRET)-based assays. The assay was conducted in triplicated using a 96-well black plate as described previously [21]. The final reaction volume included 70 µL of assay buffer (50 mM HEPES pH 7.8; 100 mM NaCl, 20 % Glycerol and 5 mM Dithiothreitol), 10 µL of HCV NS3/4 A protease (final concentration 100 nM prepared in assay buffer), 10 µL of compound, and 10 µL of RET-Substrate (final concentration 6.25 µM). The buffer, enzyme, and compound were first mixed and incubated for 15 min at 30°C. Then, the reaction began with the addition of substrate and the liberated product was continuously monitored at 30°C by measuring the fluorescence intensity (Excitation at 360 ± 10 nm and Emission 500 ± 10 nm) after each minute during 20 min using a multi-label fluorescence plate reader (BMG Labtech, Ortenberg, Germany) connected with the software CLARIOstar Mars version 3.41 to analyze the data. The initial velocity (slope of the linear section of the signal curve) was automatically deduced and expressed as Relative Fluorescence Unit per second (RFU.s^{-1}) for each compounds. Eq. (1) was used to calculate the percentage of inhibition.

$$Inhibition\,(\%) = \left(1 - \frac{Slope_{assay}}{Slope_{Control}}\right) \times 100 \quad (1)$$

Where *slope*$_{-assay}$ and *slope*$_{-control}$ are the slope of the signal curve of the reaction in presence or absence of each tested compound respectively.

2.4.2. Determination of 50 % inhibitory concentration (IC_{50}) value of the lead compounds

Only compounds that displayed over 50 % inhibition at the initial screening were tested. Their IC_{50} values were determined in the same experimental conditions as described above by using a series of expanding concentration ranging from 0 to 100 µM. The percentage of inhibition was determined for each tested concentration, and the IC_{50} value was calculated by matching the data with Eq. (2) (Hill Equation: Log [Inhibitor] vs. Response-Four parameters) using the software GraphPad Prism version 8.0.2

$$Y = I_{\max}\left(\frac{X^a}{IC_{50}^a + X^a}\right) \quad (2)$$

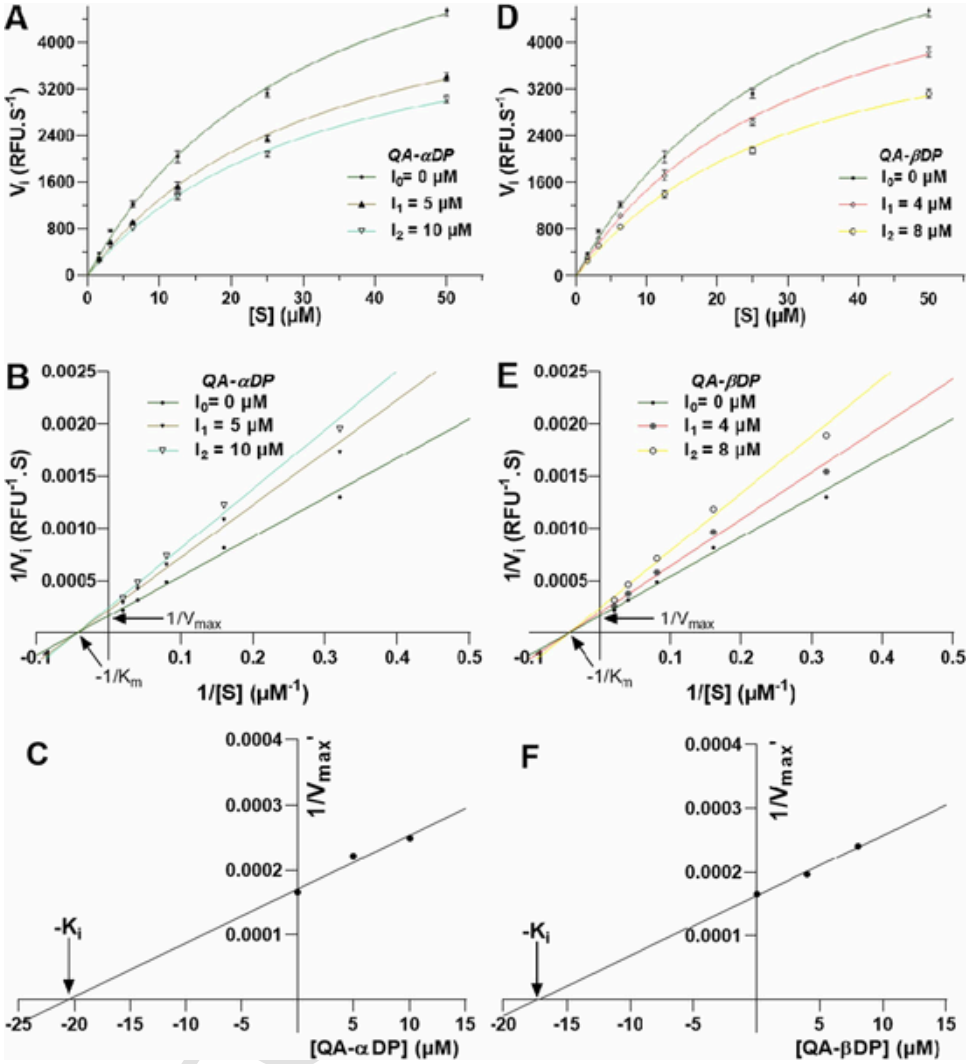

Fig. 4. Inhibition mechanism of QA-αDP and QA-βDP on the proteolytic activity of HCV NS3/4 A. A and D: Michaelis-Menten plot; B and E: Lineweaver-Burk plot; C and F: Secondary plot (1/Vmax' = f [I]) for the determination of the inhibition constant (K_i) respectively for QA-αDP and QA-βDP.

Where *Y, X* and *a* represent the percentage of inhibition, the concentration of inhibitors and the slope of the concentration-response curve (Hill slope), respectively, and I_{max} being the maximum inhibition percentage from three independent assays.

2.4.3. Determination of the inhibition mechanism of the lead compounds

The assay was conducted in the same experimental conditions as for the determination of IC_{50} by using a gradient concentration of substrate (1.5625; 3.125; 6.25; 12.5; 25 and 50 μM) and two concentrations of inhibitor (1/4 IC_{50}, 1/2 IC_{50}). The initial velocity (slope of the signal curve) in presence or absence of inhibitor was determined for each concentration of substrate and fit to Michaelis-Menten and Lineweaver-Burk equations using GraphPad Prism to unveil the mechanism of inhibition (competitive, uncompetitive, non-competitive or mixed inhibition) and the kinetics parameters (V_{max}, K_m,). In addition, the inhibition constant (K_i) of each inhibitor was determined through secondary plot ($1/V_{max}' = f[I]$) or ($K_m' = f[I]$).

2.4.4. Isothermal analysis of the interaction between HCV NS3/4 A and the isolated compounds via Thermal Shift Assay (TSA)

The interaction between the lead compounds and HCV NS3/4 A protease was carried out through TSA as described previously [21]. The assay is based on the measurement of the melting temperature of the protease in the presence or absence of the compounds. The lead compounds at 2-fold serial diluted concentrations (6.25; 12.5; 25; 50 and 100 μM) were mixed with HCV NS3/4 A protease diluted at 1 mg/mL at the proportion of 1:9 v/v, incubated (15 min, 25°C) and centrifuged (200 ×g, 25°C, 2 min). After loading the complex into capillary glass tubes, the melting temperature was recorded using a Prometheus NT48 NanoDSF apparatus through continuous increase of temperature from 25°C to 95°C at the speed of 1°C per minute. The fluorometry response was recorded at 350/330 nm.

2.4.5. Real-time binding affinity analysis of the lead compounds on HCV NS3/4 A by Surface Plasmon Resonance (SPR)

SPR binding affinity assay between the enzyme and the isolated compounds was conducted at room temperature in a Biacore™ 8k SPR System using a CM5 Sensor Chip (Cytiva) according to the instructions recommended by GE Healthcare for the analysis of small to medium size compounds. Briefly, the enzyme was prepared at 100 μM in 10 mM HEPES buffer, pH 7.4 containing 0.005 % (v/v) Tween-20 and 150 mM NaCl and immobilized on the Sensor Chip using the running buffer PBS-P (10 mM Phosphate pH 7.4; 2.7 mM KCl; 137 mM NaCl; 0.05 % Surfactant P-20). The assay running buffer (PBS-P + 5 % DMSO also used

Table 1
kinetics parameters of HCV NS3/4 A protease in presence or absence of lead compounds from *S. pobeguinii*.

Tested compounds (µM)		Michaelis-Menten Plot		Lineweaver-Burk Plot		Inhibition Mechanism	Inhibition Constant (Ki, µM)
		V_{max} (RFU/s^{-1})	K_m (µM)	V_{max} (RFU/s^{-1})	K_m (µM)		
Uninhibited reaction (I_0 = 0)		7430 ± 220	32.63 ± 3.4	6916 ± 187	22.70 ± 2.8	/	/
QA	I_1 = 4.5	6501 ± 175	32.63 ± 3.7	5265 ± 129	22.70 ± 2.5	Non-Competitive	14.22 ± 1.7
	I_2 = 9.0	4644 ± 221	32.63 ± 2.8	3760 ± 153	22.70 ± 1.5		
QA-αDP	I_1 = 5.0	5573 ± 169	32.63 ± 2.1	4512 ± 123	22.70 ± 1.8	Non-Competitive	20.56 ± 2.9
	I_2 = 10	4954 ± 198	32.63 ± 2.5	4011 ± 117	22.70 ± 2.1		
QA-βDP	I_1 = 4.0	6269 ± 174	32.63 ± 1.9	5076 ± 133	22.70 ± 1.2	Non-Competitive	17.37 ± 2.5
	I_2 = 8.0	5108 ± 209	32.63 ± 1.6	4137 ± 105	22.70 ± 1.8		
BCP	I_1 = 1.1	7099 ± 184	38.87 ± 2.5	6916 ± 117	26.73 ± 1.9	Competitive	5.15 ± 0.9
	I_2 = 2.2	5948 ± 296	44.60 ± 4.6	6916 ± 106	32.24 ± 2.6		

Values are means ± SD of three independent experiments in triplicate; **QA**: Quinovic acid; **QA-αDP**: Quinovic acid 3-O-[α-D-quinovopyranoside]; **QA-βDP**: Quinovic acid 3-O-[β-D-quinovopyranoside]; **BCP**: Boceprevir; V_{max}: Maximum reaction velocity; K_m: Michaelis-Menten constant; K_i: Inhibition Constant; I_1 and I_2: respectively low and high concentration of tested compound.

to dilute the compounds) and 4 solvent correction solutions consisting of PBS-P + 5.8 % DMSO, PBS-P + 5.3 % DMSO, PBS-P + 4.9 % DMSO and PBS-P + 4.5 % DMSO were prepared prior to flowing the compounds. These correction solutions serve as the baseline of the assay running buffer by covering a range from approximately −500 to + 1000 RU (Response Unit). Each compound at gradient concentrations (31.25; 62.5; 125; 250 and 500 µM) was flowed through the Sensor Chip surface at 50 µL/min. Data were reference with the solvent correction solutions, and sensorgrams were analyzed using the Biacore Insight Evaluation software version 2.0.15 and the Binding Models (1:1-binding kinetics model or steady-state affinity model) as well as the dissociation equilibrium constant (K_D) were determined.

2.4.6. Analysis of HCV NS3/4A-inhibitors interactions through molecular docking

The molecular basis of the interactions between the enzyme HCV NS3/4 A protease and its respective inhibitors was investigated using Molegro Virtual Docker (MVD) software as reported elsewhere [21]. The crystal structure of HCV NS3/4 A (PDB ID code: 5EQR) was retrieved from Protein Data Bank (http://www.rcsb.org) while the 2D and 3D structures of compounds were generated with Molview Software. The docking search algorithm and scoring functions were performed using the MolDock Simplex Evolution Search Algorithm and the best docking poses obtained were selected on the basis of two scoring functions: the Moldock and ReRank scores [22].

2.5. Anti-HCV activity of hit inhibitors of HCV NS3/4 A in cell-based assay

The ability of the lead compounds to inhibit HCV replication in a cell-based assay was evaluated according to the previous report [20]. Briefly, Huh7.5 cells were plated at the concentration of 6.4 × 10^3 cells/well in 96-well tissue culture plate and incubated 24 h. The medium was replaced and the cells were inoculated with the viral infectious particles deriving from Jc1/GLuc2A plasmid (HCV_{cc} at 100 $TCID_{50}$) and incubated 4 h to allow virus attachment. The inoculum was then removed, the cells washed twice using the PBS buffer and fresh medium containing various concentrations of inhibitors was added. After 72 h of incubation, the infection rate was determined by measuring the GLuc2A Luciferase activity in the incubation medium and further confirmed by the detection of HCV core protein through immunofluorescence analysis as described below.

2.5.1. Measurement of GLuc2A Luciferase activity

After the incubation period, the culture medium was collected and centrifuged (16 000 × g, 25°C, 5 min). Then, 0.25 vol of Renila 5X lysis buffer was added to the supernatants to annihilate the HCV_{cc} infectivity. Finally, the Relative Light Unit (RLU) was measured using a GLOMAX™ 20/20 Luminometer Tube Reader by injecting 20 µL of sample and 50 µL of Gaussia luciferase assay reagent, with an integration time of 10 seconds. The inhibition percentage was then calculated using Eq. (3)

$$Inhibition\,(\%) = \left(1 - \frac{RLU_{assay}}{RLU_{Control}}\right) \times 100 \quad (3)$$

Where RLU_{assay} and $RLU_{control}$ are the RLU of the supernatant in presence or absence of the inhibitor, respectively. The IC_{50} was deduced from the concentration-response curve (Log [Inhibitor] vs. Response-Three parameters) using GraphPad Prism software.

2.5.2. Immunofluorescence (IF) assay

The cells attached to the plate after 72 h were fixed in ice-cold methanol at −20°C and blocked for 30 min at room temperature with 1 % Bovine Serum Albumin in PBS. The primary antibody mouse anti-HCV core (1:1000 dilution) was added to the cells and incubated for 60 min; followed by another hour of incubation with the secondary antibody Alexa Fluor-488 Goat anti-mouse (1:1000 dilution). Finally, DAPI (4',6-diamino-2-phenylindole at 1 µg/mL) was used to stain the nucleus of the cells and images showing the cytosol of infected cells (green color) over the total number of cells (blue color) were captured using a Fluorescence Microscope.

2.6. Cytotoxic effect of selected compounds

Huh7.5 seeded at the density of 6.4 × 10^3 cells/well in 96-well tissue culture plate were incubated for 24 h. Afterward, the medium was switched with fresh medium containing the tested compounds at gradient concentrations (0–1000 µM). 72 h later, cells were washed twice with PBS and 100 µL of MTT (0.3 mg/mL in PBS) solution (3-(4, 5-dimethylthiosol-2-yl)-2, 5-diphenyl-2H-tetrazolium) was added and incubated (60 min, 37°C). The MTT solution was removed and the formazan crystals were dissolved with 100 µL of acidified isopropanol. The absorbance of the violet solution obtained was measured at 560 nm using a spectrophotometer. The percentage cell viability was then estimated using Eq. (4).

$$Cell\ viability\,(\%) = \left(\frac{Absorbance_{assay}}{Absorbance_{Control}}\right) \times 100 \quad (4)$$

Where $Absorbance_{assay}$ and $Absorbance_{control}$ are the absorbance of the dissolved formazan in presence or absence of the inhibitor, respectively. The half toxic concentration (TC_{50}) was then deduced from the concentration-response curve (Log [Inhibitor] vs. Response-Three parameters) using GraphPad Prism software. The therapeutic index (TI) of each compound was then determined as the ratio of TC_{50}/ IC_{50}.

2.7. Statistical analysis

The data are displayed as the mean ± standard deviation of three distinct assays in triplicate. One-way analysis of variance (ANOVA) was used to compare the mean values (TC_{50} or IC_{50}) between the reference

CORRECTED PROOF

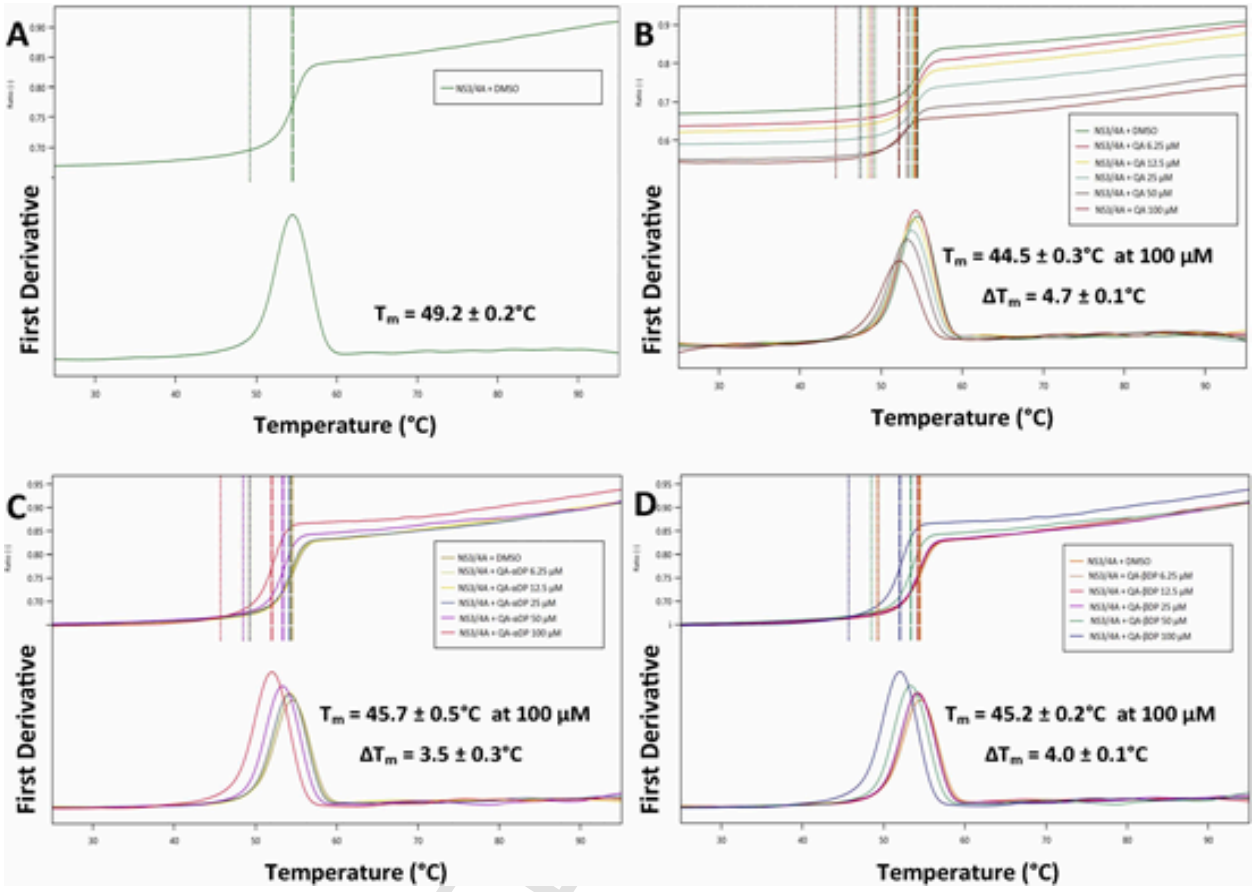

Fig. 5. Effect of lead compounds of *S. pobeguinii* on the melting temperature of HCV NS3/4 A protease. A: Melting profile of HCV NS3/4 A alone. B, C and D: Melting profile of HCV NS3/4 A in presence of increasing concentration of QA, QA-αDP and QA-βDP respectively.

inhibitor and the studied compounds. When significant differences were found between the means, Bonferroni's post hoc test was then applied. Differences between the groups under comparison were deemed significant for $P < 0.05$. The statistical program package Prism Version 8.0.2 (Graph Pad Inc., USA) was used to conduct the analyses.

3. Results

3.1. Compounds from S. pobeguinii inhibited the proteolytic activity of HCV-NS3/4 A in FRET assay

A total of 10 compounds (Fig. 1) were screened against HCV-NS3/4 A protease by continuous FRET-based enzymatic assay, followed by the determination of IC_{50} values of the best active compounds through concentration-response experiment. Fig. 2A, shows that compound **(6)**: Quinovic acid 3-O-[α-D-quinovopyranoside] (QA-αDP); compound **(8)**: Quinovic acid (QA) and compound **(9)**: Quinovic acid 3-O-[β-D-quinovopyranoside] (QA-βDP) exhibited greater than 60 % inhibition at 25 µM. Their inhibition percentages were significantly (*P<0.05*) lower when compared to Boceprevir which reached 85 % inhibition at the same concentration. Given that the other tested compounds did not reach 40 % inhibition at 25 µM, QA, QA-αDP, and QA-βDP were considered as the lead compounds. Their IC_{50} values were 20.5 ± 1.7; 18.8 ± 1.4, and 16.5 ± 1.3 µM respectively for QA-αDP (Fig. 2B); QA (Fig. 2C) and QA-βDP (Fig. 2D). Although within the micro-molar range, these IC_{50} values were significantly (*P<0.05*) higher than that of Boceprevir (IC_{50} = 4.4 ± 0.6 µM; Fig. 2E), used as reference inhibitor of HCV-NS3/4 A.

3.2. Lead compounds from S. Pobeguinii exerted non-competitive inhibition on the proteolytic activity of HCV-NS3/4 A

The type of inhibition deployed by the lead compounds against HCV-NS3/4 A protease was investigated through enzyme kinetic assay by testing each compound at 2 different concentrations (I_1 = ¼ IC_{50} and I_2 = ½ IC_{50}) alongside the uninhibited reaction (I_0 = 0 µM). The Michaelis-Menten curve (Vi = f [S]), Lineweaver-Burk plot (1/Vi = f (1/[S]) and the secondary plot (K_m' = f [I]) or 1/V_{max}' = f [I]) for each tested compound are presented in Fig. 3 and Fig. 4 and the kinetic parameters of HCV-NS3/4 A protease in presence or absence of inhibitors are presented in Table 1. For the uninhibited reaction, the approximate values of V_{max} and K_m deduced from the Michaelis-Menten curve were 7430 ± 220 RFU.s-1 and 32.63 ± 3.4 µM and the accurate values obtained from the Lineweaver-Burk representation were 6916 ± 187 RFU.s-1 and 22.70 ± 2.8 µM, respectively for V_{max} and K_m. Concerning the lead compounds from *S. pobeguinii*, the best-fit inhibition mechanism as revealed by the Lineweaver-Burk representation (series of lines with same X-axis intercept, Fig. 3B, Fig. 4B and Fig. 4E respectively for QA, QA-αDP and QA-βDP) was non-competitive inhibition. Their inhibition constant (Ki) values determined through secondary plot (1/V_{max}' = f [I]; Fig. 3C; Fig. 4C and Fig. 4F) were 14.22 ± 1.7; 20.56 ± 2.9 and 17.37 ± 2.5 µM respectively for QA, QA-αDP and QA-βDP (Table 1). In contrast, Boceprevir displayed competitive inhibition, as unveiled by the Lineweaver-Burk representation (series of lines with the same Y-axis intercept, Fig. 3E) with a Ki value of 5.15 ± 0.9 µM (Table 1) obtained from the secondary plot (Km' = f [I]; Fig. 3F).

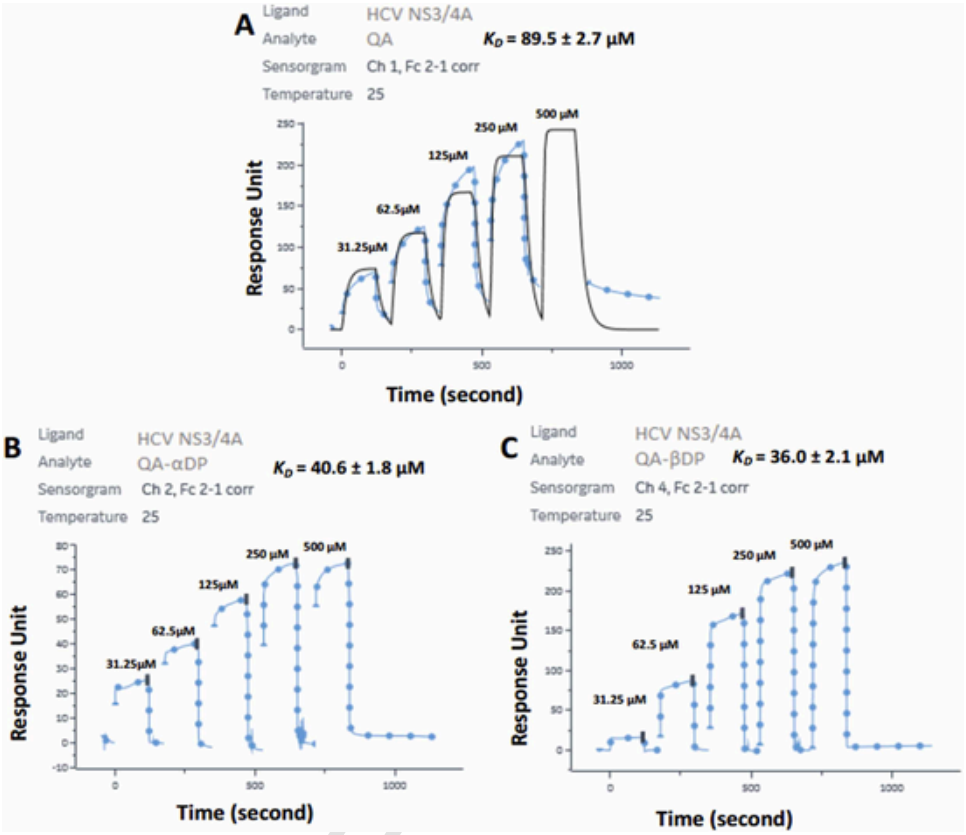

Fig. 6. Binding affinity analysis of lead compounds from *S. pobeguinii* on HCV NS3/4 A protease by SPR. A, B and C: SPR sensogram of the interaction between HCV NS3/4 A and QA, QA-αDP and QA-βDP respectively. K_D: Dissociation equilibrium constant (K_D).

3.3. Lead compounds from S. Pobeguinii decreased the melting temperature of HCV-NS3/4 A protease

Fig. 5 depicted the effect of lead compounds from *S. pobeguinii* on the melting temperature (Tm) of HCV-NS3/4 A, analyzed through Thermal Shift Assay. In the absence of an inhibitor, the Tm of HCV-NS3/4 A was 49.2°C (Fig. 5A). However, the lead compounds from *S. pobeguinii* decreased the Tm of HCV-NS3/4 A in a concentration-dependent manner. When added at 100 µM, the variation of Tm (ΔTm) was 4.7°C, 3.5°C and 4.0°C respectively, for QA (Fig. 5B), QA-αDP (Fig. 5C), and QA-βDP (Fig. 5D).

3.4. Real-time binding model of lead compounds from S. Pobeguinii on HCV-NS3/4 A protease

The binding model, as well as the dissociation equilibrium constant (K_D) between the ligands (lead compounds) and the target protein (HCV-NS3/4 A), were determined by Surface Plasmon Resonance and their sensorgrams presented in Fig. 6. QA displayed 1:1-binding kinetics model with a *KD* value of 89.5 ± 2.7 µM (Fig. 6A). However, QA-αDP (Fig. 6B) and QA-βDP (Fig. 6C) exhibited steady-state affinity model with K_D values of 40.6 ± 1.8 µM and 36.0 ± 2.1 µM, respectively.

3.5. Molecular interactions between the lead compounds from S. pobeguinii and HCV-NS3/4 A protease

The probable molecular interactions between HCV-NS3/4 A protease (PDB: 5EQR) and its respective inhibitors identified from *S. pobeguinii* were predicted by *in sillico* analysis, and the best molecular docking pose showing hydrogen bonds and steric interactions are presented in Fig. 7. The molecular docking scores (Table 2) vary from −44.08 to −94.91 Kcal/mole and from −37.51 to −39.85 Kcal/mole, respectively for MolDock and ReRank scores. These values were lower compared to those obtained with Boceprevir (-108.07 and −57.27 Kcal/mol, respectively for MolDock and ReRank scores) (Table 2). However, lead compounds from *S. pobeguinii* displayed a higher number of molecular interactions in terms of hydrogen bond and steric interactions. QA displayed a total of 9 molecular interactions (3 hydrogen bonds: 2 with His1057 and 1 with Leu1132; and 6 steric interactions: 2 with Lys1136 and 1 with both Gln1042, Phe1154, Ala1157 and Leu1135) contrary to Boceprevir with a total of 6 molecular interactions (2 hydrogen bonds with Arg1155 and 4 steric interactions: 2 with both Thr1042 and Ala1156) (Table 2).

3.6. Lead inhibitors of HCV-NS3/4 A identified from S. pobeguinii inhibited HCV replication in vitro at non-toxic concentration

As presented in Fig. 8A, QA, QA-αDP and QA-βDP did not significantly ($P > 0.05$) decrease the cell viability when tested at up-to 100 µM, contrary to Boceprevir which reduced the cell viability from 100 % to 80 % at the same concentration. The TC_{50} values for QA, QA-αDP, QA-βDP and Boceprevir were 685.4; 739.5; 707.9 and 204.7 µM respectively.

The GLuc2A luciferase Reporter virus assay showed that the tested compounds exhibited a concentration-dependent inhibitory effect. Their IC_{50} values deduced from the concentration-response curve and the therapeutic index (TI) calculated as ratio of TC_{50}/IC_{50} were 46.53 ± 2.18 µM and 19; 40.33 ± 1.83 µM and 19; 34.91 ± 2.71 µM and 23; and 2.77 ± 0.6 µM and 73, respectively for QA (Fig. 8B), QA-αDP (Fig.

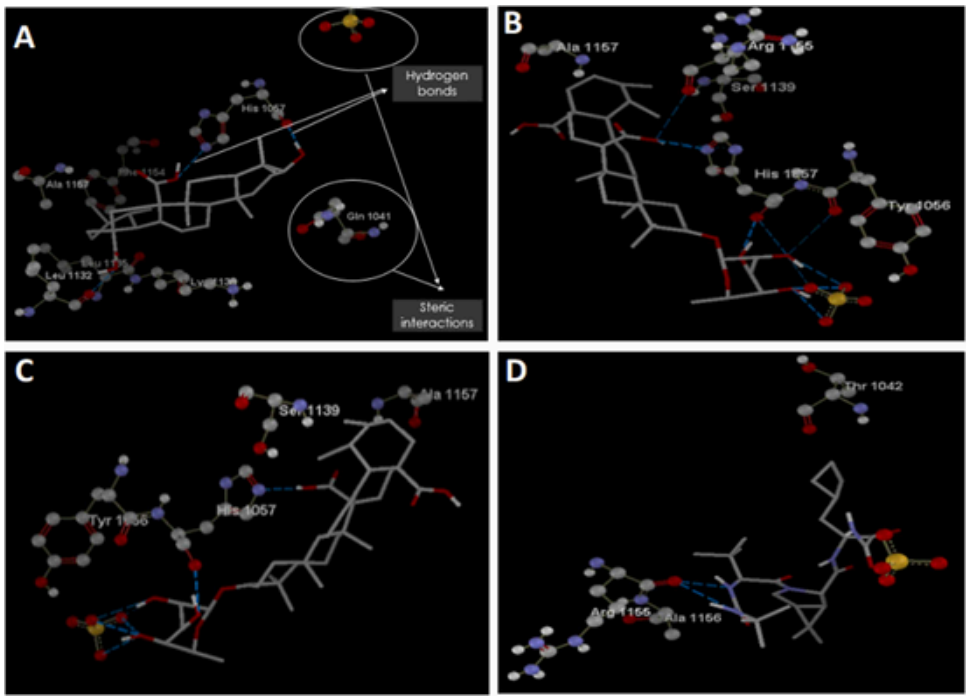

Fig. 7. Molecular docking analysis of the interactions between lead compounds from S. pobeguinii and HCV NS3/4 A (PDB: 5EQR). (A), (B), (C) and (D): Predicted molecular binding poses between 5EQER and QA, QA-αDP, QA-βDP and Boceprevir respectively.

Table 2
Molecular Docking Scores and type of interactions between lead compounds from *S. pobeguinii* and HCV NS3/4 A (PDB: 5EQR).

Ligands	HCV NS3/4 A (5EQR)			
	MolDock Score (Kcal/mol)	ReRank Score (Kcal/mol)	Type of interactions	
			Hydrogen bond	Steric interaction
QA	−94.9146	−37.5191	**3 interactions:** 2 with His1057 1 with Leu1132	**6 interactions:** 1 with Gln1041 2 with Lys1136 1 with Phe1154 1 with Ala1157 1 with Leu1135
QA-αDP	−44.0847	−38.1442	**3 interactions:** 1 with Arg1155 1 with His1057 1 with Tyr1056	**6 interactions:** 2 with Ser1139 1 with Ala1157 3 with His1057
QA-βDP	−44.3692	−39.858	**1 interaction:** 1 with His1057	**5 interactions:** 1 with Ser1139 1 with Ala1157 2 with His1057 1 with Tyr1056
BCP	−108.072	−57.2749	**2 interactions:** 2 with Arg1155	**4 interactions:** 2 with Thr1042 2 with Ala1156

8C) and QA-βDP (Fig. 8 D) and Boceprevir (Fig. 8E). When tested at 50 μM, the inhibitory activity of the lead compounds from *S. pobeguinii* was comparable to that of Boceprevir, as illustrated by IFA (Fig. 9).

4. Discussion

The coronavirus's papain- or chymotrypsin-like protease proves that viral proteases are known to be crucial to the lifecycle of viruses [21, 23]. It is also the case for the HCV-NS3/4 A protease, a bifunctional protease that exhibits both helicase and serine-protease activities [6]. Indeed, following host cell infection by the HCV, its genome codes for a precursor polyprotein, which is processed by viral and host cell enzymes into ten functional proteins [5,24], and HCV-NS3/4 A protease is necessary to cleave at least four junctions in the polyprotein [6,9]. In addition, HCV-NS3/4 A protease is essential for immune system evasion, primarily through reducing interferon, pro-inflammatory cytokines, and antiviral proteins production. [7,8]. Due to these crucial functions, targeting the HCV-NS3/4 A protease is an efficient strategy to combat HCV infection. Out of the ten compounds from *S. pobeguinnii* examined as possible inhibitors of HCV-NS3/4 A's proteolytic activity, three of them, known as Quinovic acid (QA), Quinovic acid 3-O-[α-D-quinovopyranoside] (QA-αDP), and Quinovic acid 3-O-[β-D-quinovopyranoside] (QA-βDP), alongside Boceprevir, used as a reference inhibitor, were found to display outstanding concentration-dependent inhibitory activity at the micromolar range (Fig. 2). The ability of QA, QA-αDP, and QA-βDP to suppress the proteolytic activity of HCV-NS3/4 A protease implies that they can function as direct-acting antiviral inhibitors against HCV infection.

Enzyme kinetics experiments were carried out in order to define the mechanism of inhibition of these lead compounds. The results showed that, contrary to Boceprevir, which displayed a competitive inhibition (Lineweaver-Burk plot, Fig. 3E) with an inhibition constant (K_i) value of 5.15 μM (Table 1), the best-fit inhibition model appeared to be a non-competitive inhibitor for both QA (Fig. 3B), QA-αDP (Fig. 4B), and QA-βDP (Fig. 4E) with K_i values of 14.22, 20.56, and 17.37 μM (Table 1), respectively. These observations indicate Boceprevir decreases the affinity of the substrate to the enzyme (K_m) through direct binding to the substrate binding site of the enzyme or modification of its structural conformation, while lead compounds from *S. pobeguinii* reduce the maximum reaction velocity (V_{max}) without affecting K_m. These findings suggest that QA, QA-αDP, or QA-βDP do not bind to the free enzyme but rather bind to the enzyme-substrate complex and subsequently decrease V_{max}. Compared to competitive inhibitors like Boceprevir, whose inhibitory ability can be annihilated by an excess quantity of substrate, these non-competitive inhibitors may be preferable, given that they bind on the enzyme-substrate complex.

CORRECTED

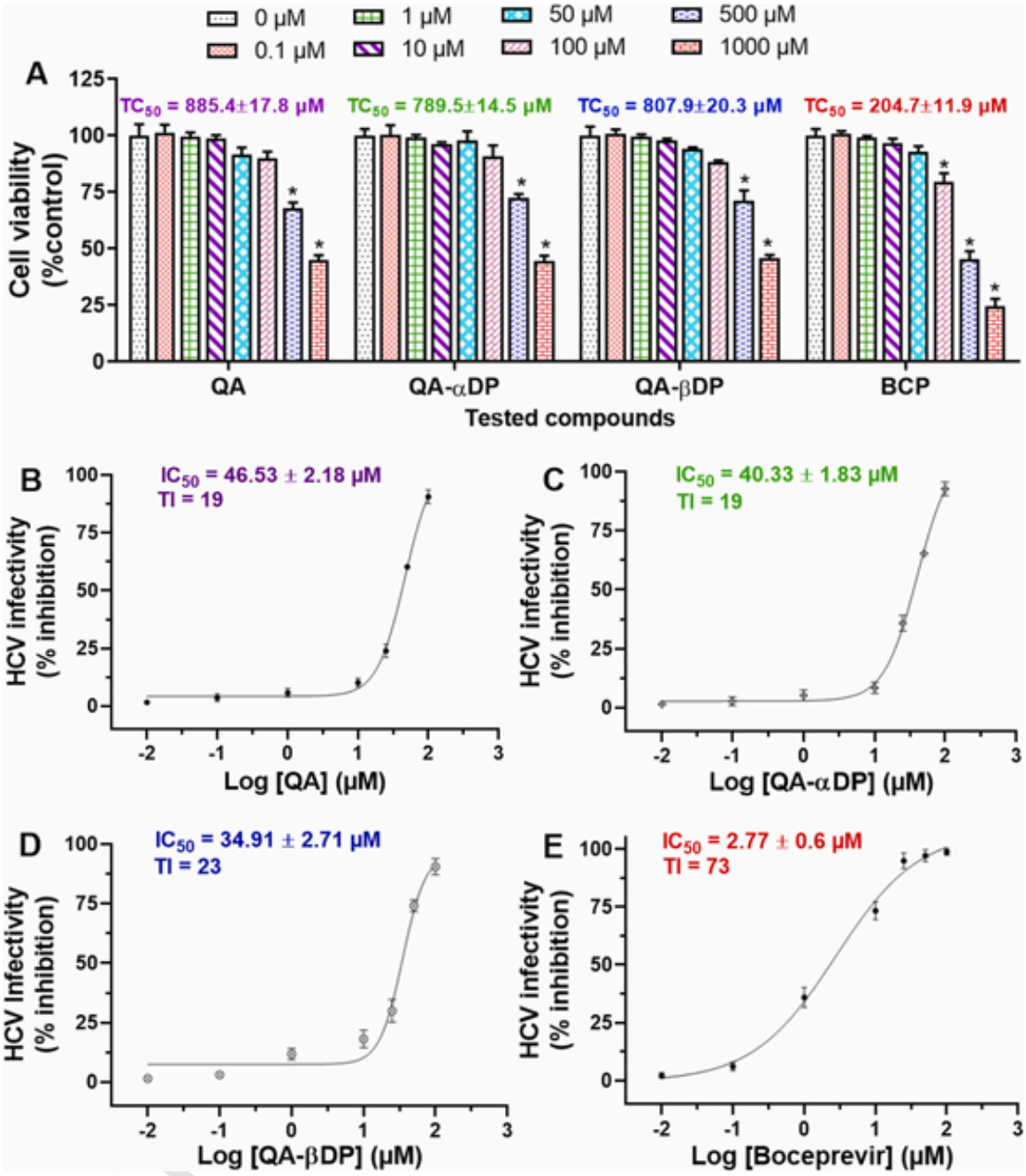

Fig. 8. Anti-HCV activity and cytotoxicity effect of lead compounds from *S. pobeguinii* on Huh7.5 cells. Cells were incubated without (control) or with increasing concentrations of tested compounds and the cellular viability (A) expressed as percentage of control was measured 72 h later. Huh7.5 cells were infected with HCVcc for 4 h, then the medium was replaced and cells were incubated with or without (control) various concentrations of compounds. 72 h later, the activity of Gluc2A (Relative Light Units [RLU]) was measured in the incubation medium, and the percentage of inhibition was determined. For each tested compound, the TC_{50} or IC_{50} was determined from the concentration-response curve and the TI was deduced as ration of TC_{50}/IC_{50}. **(B)**, **(C)**, **(D)** and **(E)**: Inhibitory effect of QA, QA-αDP, QA-βDP and Boceprevir respectively. Data are means ± SD of three independent assays in triplicate; *(n = 3)(n = 3)*. ANOVA summary: F(DFn, DFd) = F(7, 16) = 132.8, P<0.0001 (QA, Fig. 2**A**); F(DFn, DFd) = F(7, 16) = 120.0, P<0.0001 (QA-αDP, Fig. 2**A**); F(DFn, DFd) = F(7, 16) = 201.9, P<0.0001 (QA-βDP, Fig. 2**A**); F(DFn, DFd) = F(7, 16) = 171.1, P<0.0001 (BCP, Fig. 2**A**);.*values significantly (P<0.05) different when compared to control group (0 µM) using Bonferroni's test. TI (TC_{50}/IC_{50}): Therapeutic index; TC_{50}: 50 % toxic concentration; IC_{50}: 50 % inhibitory concentration.

Furthermore, two innovative techniques were then employed to characterize the physical interactions between HCV-NS3/4 A and its inhibitors. On the one hand, Differential Scanning Fluorometry, also known as Thermal Shift Assay [25], demonstrated that QA, QA-αDP, or QA-βDP considerably decreased the melting temperature (HCV-NS3/4 A) in a concentration-dependent manner (Fig. 5). These results are consistent with a previous report showing that flavonoids from *Crinum distinchum* effectively inhibited the proteolytic and deubiquinating activities of the papain-like protease of coronavirus by decreasing its melting temperature [21]. On the other hand, surface plasmon resonance revealed that QA displayed a 1:1 binding kinetics model with a dissociation equilibrium constant (K_D) value of 89.5 µM toward HCV-NS3/4 A (Fig. 6A), while QA-αDP (Fig. 6B) and QA-βDP (Fig. 6C) exhibited a steady-state binding affinity model with the respective K_D values

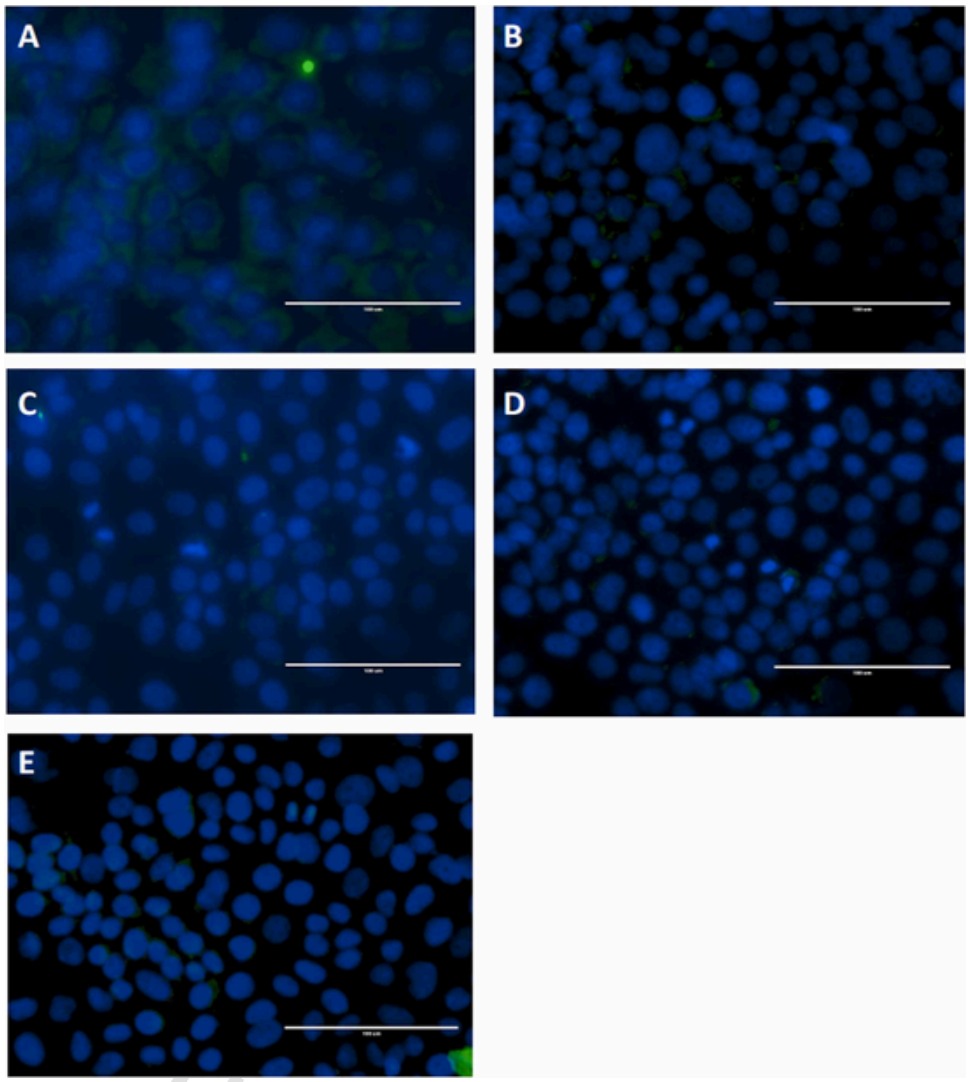

Fig. 9. Influence of lead compounds from *S. pobeguinii* on the detection of HCV Core protein in infected Huh7.5 cells. Huh7.5 cells were infected with HCVcc for 4 h, then the medium was replaced and cells were incubated without (control) or with 50 μM of each tested compounds. 72 h later, HCV core protein detection was detected in infected cells through immunofluorescence analysis and images showing HCV core protein (green color) surrounding the nucleus (blue color) of cells were recorded using a fluorescence microscope. **(A)**: Control group (infected and non-treated). **(B)**, **(C)**, **(D)** and **(E)**: Inhibitory effect of QA, QA-αDP**,** QA-βDP and Boceprevir respectively.

of 40.6 and 36.0 μM. The difference observed between the two binding modes could be due to the presence of the glycoside residue (-D-quinovopyranoside) in the chemical structure of QA-αDP or QA-βDP. Taken together, these results demonstrate that QA and its derivatives effectively bind to the HCV-NS3/4 A protease, destabilizing its native structure and consequently inhibiting its proteolytic activity.

The molecular basis of the interactions between HCV-NS3/4 A and its inhibitors from *S. pobeguinii* was also predicted through a computational approach (Fig. 7). Globally, the docking scores (Moldock and ReRanK scores) obtained with QA, QA-αDP, or QA-βDP were slightly lower than those obtained with Boceprevir (Table 2). However, they all displayed more interactions with amino acid residues when compared to Boceprevir. Indeed, only 6 interactions (2 hydrogen bonds with Arg1155 and 4 steric interactions: 2 with Thr1042 and 2 with Ala 1156) were observed between Boceprevir and HCV-NS3/4 A enzyme, while up to 9 molecular interactions (3 hydrogen bonds: 1 with Arg 1155, His1057, and Tyr1056, and 6 steric interactions: 1 with Ala 1157, 2 with Ser1139, and 3 with His1057) were found between QA-αDP and HCV-NS3/4 A protease. These results suggest that the decrease in HCV-NS3/4 A's melting temperature as well as the various binding affinity models observed between the lead compounds from *S. pobeguinii* and HCV-NS3/4 A can be imputed to these molecular interactions, which may effectively impede the native conformation of the enzyme and subsequently decrease its proteolytic activity.

The efficacy of the identified inhibitors of HCV-NS3/4 A protease from *S. pobeguinii* to inhibit HCV replication was further examined in a cell-based assay, alongside their cytotoxicity in the Huh7.5 cell line, which serves as the host cell. As illustrated by the MTT assay and Luciferase reporter assay (Fig. 8) and immunofluorescence analysis (Fig. 9), QA, QA-αDP, and QA-βDP effectively inhibited *in vitro* replication of HCV in Huh7.5 cells line, and their inhibitory effect was comparable to that of Boceprevir at 50 μM. Although we previously demonstrated the anti-proliferative activity of these compounds against various cancer cells line including MCF-7: human breast adenocarcinoma cells; HepG2: human hepatocellular carcinoma cells, and A549: human epithelial lung adenocarcinoma cells [17], they were less toxic for the Huh7.5 cells line used in this study, with a TC_{50} greater than 650 μM, which was significantly ($P^{<}0.05$) different to that of Boceprevir (TC_{50}

CORRE

= 204 μM). Here, the effectively inhibited the *in vitro* replication of HCV in Huh7.5 cells at non-toxic concentrations. These findings suggest that the tested inhibitors are relatively safe for the host cells and may block HCV replication through the inhibition of the proteolytic activity of HCV-NS3/4 A. These results are also in agreement with previous reports where inhibitors of HCV-NS3/4 A were effective in blocking *in vitro* replication of HCV [26,27]. Consistent with previous findings, our study confirmed that *S. pobeguinii* is a reservoir of phytochemical compounds with various pharmacological activities. Indeed, the antioxidant, anti-inflammatory and anti-cancer properties of compounds and extracts from *S. pobeguinii* have been demonstrated [16,17]. Here, we reported for the first time, its antiviral properties. However, all these reported pharmacological activities have been established using *in vitro* systems. It is therefore necessary to conduct further experiments in animal models, including the exploration of pharmacokinetics and bioavailability of the studied compounds to not only validate the observed activities, but also to evaluate the clinical relevance and applicability of these compounds. In addition, if promising activities are obtained in vivo, the exploration of large-scale extraction or hemisynthesis of these compounds can be considered.

5. Conclusion

The present study examined the ability of compounds isolated from *S. pobeguinii* to inhibit the proteolytic activity of the HCV-NS3/4 A protease. Three compounds: Quinovic acid (QA), Quinovic acid 3-O-[α-D-quinovopyranoside] (QA-αDP), and Quinovic acid 3-O-[β-D-quinovopyranoside] (QA-βDP) were successfully identified as inhibitors of HCV-NS3/4 A. They displayed their inhibitory activity towards HCV-NS3/4 A through a non-competitive inhibition mechanism. In addition, these inhibitors bound to the HCV-NS3/4 A protease in a real-time manner, inducing its instability by lowering its melting temperature. Furthermore, the lead compounds effectively inhibited HCV replication in a cell-based assay at a non-toxic concentration. Globally, these results contribute to the valorization of *S. pobeguinii* as a potential source of efficient inhibitors to reinforce the current therapeutic arsenal for the treatment of HCV infection.

Funding

This work was supported by the Chinese Academy of Sciences President International Fellowship Initiative (CAS-PIFI) [grant number: P00019].

CRediT authorship contribution statement

Jules Clément Nguedia Assob: Writing – review & editing, Visualization, Validation, Supervision, Software, Resources, Formal analysis. **Pierre Mkounga:** Writing – review & editing, Visualization, Validation, Software, Resources, Methodology, Conceptualization. **Armel Jackson Seukep:** Writing – review & editing, Visualization, Validation, Methodology, Investigation, Data curation. **Felicité Syntia Douanla Somene:** Writing – review & editing, Writing – original draft, Methodology, Investigation, Formal analysis. **Brice Fredy Nemg Simo:** Writing – review & editing, Visualization, Software, Resources, Investigation, Formal analysis. **Armelle Gaelle Kwesseu Fepa:** Writing – original draft, Investigation, Formal analysis, Data curation. **Elisabeth Menkem Zeuko'o:** Writing – review & editing, Visualization, Validation, Supervision, Methodology, Investigation, Formal analysis. **Jordas Casares Tchana Tchamba:** Writing – original draft, Visualization, Software, Methodology, Investigation, Formal analysis. **Aristide Mfifen Munvera:** Writing – review & editing, Writing – original draft, Software, Resources, Methodology, Investigation, Formal analysis, Conceptualization. **Paul Fewou Moundipa:** Writing – review & editing, Visualization, Validation, Supervision, Resources, Project administration, Formal analysis, Conceptualization. **Arnaud Fondjo Kouam:** Writing – review & editing, Writing – original draft, Validation, Software, Resources, Project administration, Methodology, Investigation, Funding acquisition, Formal analysis, Data curation, Conceptualization. **Frédéric Nico Njayou:** Writing – review & editing, Visualization, Validation, Supervision, Resources, Formal analysis, Data curation, Conceptualization.

Declaration of Competing Interest

The authors declare that they have no known competing financial interests or personal relationships that could have appeared to influence the work reported in this paper.

Acknowledgments

The authors thank the Institute of Microbiology, Chinese Academy of Sciences, Beijing-China for providing core facilities to carry out SPR experiments.

Supplementary material

Slope of signal curve based on raw data generated automatically by the software CLARIOstar Mars version 3.41 and used to determine the IC_{50} of lead compounds.

Data availability

All data generated or analyzed during this study are included in this published article and its supplementary information files

Appendix A. Supporting information

Supplementary data associated with this article can be found in the online version at doi:10.1016/j.prerep.2024.100026.

References

[1] W.H.O., Hepatitis C: who.int/news-room/fact-sheets/detail/hepatitis-c, (2023). ⟨https://www.who.int/news-room/fact-sheets/detail/hepatitis-c⟩ (Accessed March 27, 2024).
[2] N. Salari, M. Kazeminia, N. Hemati, M. Ammari-Allahyari, M. Mohammadi, S. Shohaimi, Global prevalence of hepatitis C in general population: a systematic review and meta-analysis, Travel Med. Infect. Dis. 46 (2022) 102255, https://doi.org/10.1016/j.tmaid.2022.102255.
[3] R. Bartenschlager, S. Sparacio, Hepatitis C virus molecular clones and their replication capacity in vivo and in cell culture, Virus Res. 127 (2007) 195–207, https://doi.org/10.1016/j.virusres.2007.02.022.
[4] D. Moradpour, F. Penin, C.M. Rice, Replication of hepatitis C virus, Nat. Rev. Microbiol. 5 (2007) 453–463, https://doi.org/10.1038/nrmicro1645.
[5] T.L. Tellinghuisen, C.M. Rice, Interaction between hepatitis C virus proteins and host cell factors, Curr. Opin. Microbiol. 5 (2002) 419–427, https://doi.org/10.1016/S1369-5274(02)00341-7.
[6] C. Lin, H.C.V. NS3-4A Serine Protease, in: S.-L. Tan (Ed.), Hepat. C Viruses Genomes Mol. Biol., Horizon Bioscience, Norfolk (UK), 2006. http://www.ncbi.nlm.nih.gov/books/NBK1623/ (Accessed July 22, 2024).
[7] A.R. Ferreira, B. Ramos, A. Nunes, D. Ribeiro, Hepatitis C Virus: Evading the Intracellular Innate Immunity, J. Clin. Med. 9 (2020) 790, https://doi.org/10.3390/jcm9030790.
[8] C. Xu, J. Chen, X. Chen, Host innate immunity against hepatitis viruses and viral immune evasion, Front. Microbiol. 12 (2021), https://doi.org/10.3389/fmicb.2021.740464.
[9] F. Butt, M. Shahid, M. Hassan, F. Tawakkal, I. Amin, S. Afzal, R. Bhatti, R. Nawaz, M. Idrees, A review on hepatitis C virus: role of viral and host-cellular factors in replication and existing therapeutic strategies, Egypt. Liver J. 12 (2022) 71, https://doi.org/10.1186/s43066-022-00232-w.
[10] R. De Francesco, C. Steinkühler, Structure and function of the hepatitis C virus NS3-NS4A serine proteinase, in: C.H. Hagedorn, C.M. Rice (Eds.), Hepat. C Viruses, Springer, Berlin, Heidelberg, 2000, pp. 149–169, https://doi.org/10.1007/978-3-642-59605-6_8.
[11] D.B.S. Brashier, S. Sharma, A.G. Mathur, P. Khare, S. Gupta, Boceprevir: a new hope against hepatitis C virus, J. Pharmacol. Pharmacother. 3 (2012) 213–215, https://doi.org/10.4103/0976-500X.95548.
[12] S. Bruno, J.M. Vierling, R. Esteban, L.M. Nyberg, H. Tanno, Z. Goodman, F.

CORRECTED PROOF

Poordad, B. Bacon, K. Gottesdiener, L.D. Pedicone, J.K. Albrecht, C.A. Brass, S. Thompson, M.H. Burroughs, Efficacy and safety of boceprevir plus peginterferon-ribavirin in patients with HCV G1 infection and advanced fibrosis/cirrhosis, J. Hepatol. 58 (2013) 479–487, https://doi.org/10.1016/j.jhep.2012.11.020.

[13] M. Miao, X. Jing, E. De Clercq, G. Li, Danoprevir for the treatment of hepatitis C virus infection: design, development, and place in therapy, Drug Des. Devel. Ther. 14 (2020) 2759–2774, https://doi.org/10.2147/DDDT.S254754.

[14] M.S. Sulkowski, K.E. Sherman, D.T. Dieterich, M. Bsharat, L. Mahnke, J.K. Rockstroh, S. Gharakhanian, S. McCallister, J. Henshaw, P.-M. Girard, B. Adiwijaya, V. Garg, R.A. Rubin, N. Adda, V. Soriano, Combination therapy with telaprevir for chronic hepatitis C virus genotype 1 infection in patients with HIV: a randomized trial, Ann. Intern. Med. 159 (2013) 86–96, https://doi.org/10.7326/0003-4819-159-2-201307160-00654.

[15] R.J.O. Barnard, J.A. Howe, R.A. Ogert, S. Zeuzem, F. Poordad, S.C. Gordon, R. Ralston, X. Tong, V. Sniukiene, J. Strizki, D. Ryan, J. Long, P. Qiu, C.A. Brass, J. Albrecht, M. Burroughs, S. Vuocolo, D.J. Hazuda, Analysis of boceprevir resistance associated amino acid variants (RAVs) in two phase 3 boceprevir clinical studies, Virology 444 (2013) 329–336, https://doi.org/10.1016/j.virol.2013.06.029.

[16] E. Mfotie Njoya, A.M. Munvera, P. Mkounga, A.E. Nkengfack, L.J. McGaw, Phytochemical analysis with free radical scavenging, nitric oxide inhibition and antiproliferative activity of Sarcocephalus pobeguinii extracts, BMC Complement. Altern. Med. 17 (2017) 199, https://doi.org/10.1186/s12906-017-1712-5.

[17] E. Mfotie Njoya, B. Ndemangou, J. Akinyelu, A.M. Munvera, ChikaI. Chukwuma, P. Mkounga, S.S. Mashele, T.J. Makhafola, L.J. McGaw, In vitro antiproliferative, anti-inflammatory effects and molecular docking studies of natural compounds isolated from Sarcocephalus pobeguinii (Hua ex Pobég), Front. Pharmacol. 14 (2023) 1205414, https://doi.org/10.3389/fphar.2023.1205414.

[18] B.D. Lindenbach, M.J. Evans, A.J. Syder, B. Wolk, T.L. Tellinghuisen, C.C. Liu, T. Maruyama, R.O. Hynes, D.R. Burton, J.A. McKeating, C.M. Rice, Complete replication of hepatitis C Virus in cell culture, Science 309 (2005) 5.

[19] T. Phan, R.K.F. Beran, C. Peters, I.C. Lorenz, B.D. Lindenbach, Hepatitis C virus NS2 protein contributes to virus particle assembly via opposing epistatic interactions with the E1-E2 glycoprotein and NS3-NS4A enzyme complexes, J. Virol. 83 (2009) 8379–8395, https://doi.org/10.1128/JVI.00891-09.

[20] A.F. Kouam, F.N. Njayou, F. Yuan, B.O. Oladejo, H. Hongtao, P. Mkounga, P.F. Moundipa, Inhibitory activity of limonoids from Khaya grandifoliola C.DC (Meliaceae) against hepatitis C virus infection in vitro, Avicenna J. Phytomedicine 11 (2021) 353–366, https://doi.org/10.22038/AJP.2020.17215.

[21] A.F. Kouam, F.D. Mabou, L. Fu, R.R. Koagne, Y. Li, B.A. Owona, E.M. Zeuko'o, A.G.K. Fepa, B.R.T. Galani, F. Reyes, F.N. Njayou, P.F. Moundipa, G.F. Gao, Insights into the inhibition mechanisms of MERS-CoV and SARS-CoV2 papain-like proteases by inhibitors from *Crinum distichum: In vitro* and *in silico* analysis, South Afr. J. Bot. 165 (2024) 290–306, https://doi.org/10.1016/j.sajb.2024.01.004.

[22] G. Bitencourt-Ferreira, W.F. de Azevedo, Molegro virtual docker for docking, Methods Mol. Biol. Clifton NJ 2053 (2019) 149–167, https://doi.org/10.1007/978-1-4939-9752-7_10.

[23] V. Kumar, K.-P. Tan, Y.-M. Wang, S.-W. Lin, P.-H. Liang, Identification, synthesis and evaluation of SARS-CoV and MERS-CoV 3C-like protease inhibitors, Bioorg. Med. Chem. 24 (2016) 3035–3042, https://doi.org/10.1016/j.bmc.2016.05.013.

[24] R. Bartenschlager, F.-L. Cosset, V. Lohmann, Hepatitis C virus replication cycle, J. Hepatol. 53 (2010) 583–585, https://doi.org/10.1016/j.jhep.2010.04.015.

[25] B. Baljinnyam, M. Ronzetti, A. Yasgar, A. Simeonov, Applications of differential scanning fluorometry and related technologies in characterization of protein–ligand interactions, in: N.E. Labrou (Ed.), Target. Enzym. Pharm. Dev. Methods Protoc., Springer US, New York, NY, 2020, pp. 47–68, https://doi.org/10.1007/978-1-0716-0163-1_4.

[26] S.M. El-Sayed, M.A.M. Ali, B.E.-D.M. El-Gendy, S.S. Dandash, Y. Issac, R. Saad, M.M. Azab, M.R. Mohamed, Identification of novel small molecule inhibitors against the NS3/4A protease of hepatitis C virus genotype 4a, Curr. Pharm. Des. 24 (2018) 4484–4491, https://doi.org/10.2174/1381612825666181203153835.

[27] I. Meewan, X. Zhang, S. Roy, C. Ballatore, A.J. O'Donoghue, R.T. Schooley, R. Abagyan, Discovery of new inhibitors of hepatitis C Virus NS3/4A protease and its D168A mutant, ACS Omega 4 (2019) 16999–17008, https://doi.org/10.1021/acsomega.9b02491.

CORRECTED PROOF

View publication stats